Investigating static liquefaction as a potential mode of failure for Edenville dam via numerical simulation

Vincent Castonguay
Seequent, Calgary, AB, Canada

GeoCalgary 2022 October 2-5 Reflection on Resources

ABSTRACT
On May 19th, 2020, Edenville Dam (Michigan) failed after the area was subjected to intense rainfall. An independent forensic team (IFT) released a preliminary report in which three probable causes of failure are identified. The IFT considers static liquefaction of the embankment to be the most probable cause of failure. The objective of this paper is to perform a simple investigation of static liquefaction as a potential mode of failure for Edenville dam. The SIGMA/W software (GeoStudio) is used to simulate the rise of reservoir level during the rainfall and its impact on the overall stability of the dam. The NorSand constitutive model is used to model the dam body. While many hypotheses are made to conduct this simplified study, the simulation results nevertheless show that static liquefaction of the dam is indeed possible as a direct consequence of the rapid increase in reservoir level.

RÉSUMÉ
Le 19 mai 2020, le barrage Edenville (Michigan) s'est rompu après que la région eut été soumise à des précipitations intenses. Une équipe d'enquête indépendante (EEI) a publié un rapport préliminaire dans lequel trois causes de rupture probables sont identifiées. L'EEI considère que la liquéfaction statique du barrage est la cause la plus probable de la rupture. L'objectif de cet article est de réaliser une étude simplifiée de la liquéfaction statique comme mode potentiel de rupture du barrage Edenville. Le logiciel SIGMA/W (GeoStudio) est utilisé pour simuler l'élévation du niveau du réservoir pendant les précipitations et son impact sur la stabilité globale du barrage. La loi de comportement NorSand est utilisée pour modéliser le corps du barrage. Malgré les nombreuses hypothèses avancées pour réaliser cette étude simplifiée, les résultats des simulations montrent néanmoins que la liquéfaction statique du barrage est effectivement possible en conséquence directe de l'augmentation rapide du niveau du réservoir.

1 INTRODUCTION

On May 19th, 2020, Edenville Dam (Michigan) failed after the area was subjected to intense rainfall. The failure of Edenville dam caused the water stored in Wixom Lake (the reservoir behind the dam) to be released in an uncontrolled way. The residential area downstream of the dam was inundated, which caused important material damage. An independent forensic team (IFT, France *et al.*, 2021) released a preliminary report in September 2021 in which three probable causes of failure are identified. The IFT considers static liquefaction of the embankment to be the most probable cause of failure.

The objective of this paper is to perform a simple investigation of static liquefaction as a potential mode of failure for Edenville dam via numerical simulation. The stress-strain numerical simulation package SIGMA/W from the GeoStudio suite is used to simulate the rise of reservoir level during the rainfall event and its impact on the overall stability of the dam. The NorSand constitutive model is used to model the dam body. The input parameters for the model are adjusted using drained and undrained triaxial compression test results available in the IFT preliminary report.

An important aspect that defines this study is to only use the limited information made available by the IFT to carry out the numerical simulations. This is done purposely. The desired goal is to demonstrate how interesting conclusions can be drawn from analyses performed with such limited data. Static liquefaction of Edenville dam is shown to be possible as a result of the increase in pore-water pressure following the intense rainfall event.

2 EDENVILLE DAM

Edenville Dam was constructed in the mid-1920s as part of a power generation facility. The IFT reports construction methods would likely have included material dumping, without proper compaction. This element is key to the discussion that follows.

2.1 Dam geometry

The dam is approximately 190 m long. According to the original design plans, the upstream and downstream slopes were 2:5H:1V and 2H:1V respectively. However, the IFT reports recent surveys indicating steeper slopes than originally built in many sections of the dam. In the vicinity of the dam failure, the dam was approximately 9.5 m high, with a crest width of approximately 3.5 m.

2.2 Embankment material and foundation

Near the dam failure, the IFT reports the embankment was made of loose uniform fine sand (low blow counts were measured during *in situ* investigations). The embankment is founded on a dense sand layer with varying amounts of silt, which overlays a clayey glacial till deposit. The IFT report doesn't include much more in terms of *in situ* soil characterization.

2.3 Edenville dam failure

While Endenville dam failed on May 19th, 2020, the rainfall event leading to the failure began the day before, on May 18th. During these two days, approximately 9.6 cm of

rainfall was registered at the dam location. The rainfall event affected a very large region upstream of the dam, which resulted in a very significant reservoir level increase. According to the IFT, the Edenville reservoir level increased by approximately 1.8 m in the two days leading to the failure, from elevation 205.86 m (0.12 m below the normal pool level) to elevation 207.66 m. This was 0.9 m beyond the previous pool of record of 206.75 m set in 1929.

As the reservoir pool began to rise on May 18th, all six spillway gates located close to Edenville dam were eventually opened and remained so until the dam failed on May 19th at 5:35 pm.

3 NUMERICAL SIMULATION SETUP

The GeoStudio numerical simulation software suite (Seequent, 2022) was used to run the 2D simulations presented hereafter. The modelling sequence used employed the SEEP/W and SIGMA/W modules, following a four-step workflow:

1. Establish seepage conditions in the domain before the start of the rainfall event.
2. Establish effective stress conditions before the start of the rainfall event.
3. Perform stress correction to eliminate ill-conditioned stresses in the domain.
4. Calculate the fully coupled stress-strain response of the dam during the rainfall event.

The specific GeoStudio modules and analysis types used are laid out in Table 1.

Table 1. Simulation steps in GeoStudio

Simulation step		GeoStudio module	Analysis type
1.	Initial seepage conditions	SEEP/W	Steady-state seepage
2.	Initial stresses	SIGMA/W	*In situ* gravity activation
3.	Stress correction	SIGMA/W	Stress correction
4.	Rainfall event	SIGMA/W	Consolidation

The stress correction routine performed in step 3 was specifically designed for this paper. Its objective was to only eliminate areas where negative mean effective stresses (tension) arose following the gravity activation phase (step 2). The submerged toe of a dam-like geometry can be particularly vulnerable to such ill-conditioned stresses and must be corrected before performing stress-strain analyses.

A consolidation analysis is used in step 4 of the modelling process. This analysis type allows for fully coupled stress-strain – water transfer simulations. This type of analysis automatically considers materials to become undrained to allow for the simulation of the evolution of pore-water pressure throughout the domain. 75 calculations steps are used to integrate the boundary conditions presented in section 3.2.

3.1 Model geometry and meshing

The model geometry used replicates the description made in section 2.1 and is shown in Figure 1. Quadrilateral finite elements with secondary nodes (a total of eight calculation nodes per element) were used. The finite elements have an approximate size of 0.6 m. Elements are allowed to be twice this size near the edges of the domain to reduce the number of calculation nodes. Secondary nodes are turned off in the upper portion of the dam geometry to allow for faster solve times in the unsaturated zone, where more limited deformations are expected.

3.2 Boundary conditions

The boundary conditions used for the simulations are shown in Figure 1 and summarized in Table 2.

Table 2. Boundary conditions applied to the domain

Boundary condition type	Location
Fix X and Y	Bottom of the domain
Fix X	Left and right edges of the domain
Water total head	Upstream of the dam
Hydrostatic pressure	Upstream of the dam
Water flux + seepage	Downstream of the dam

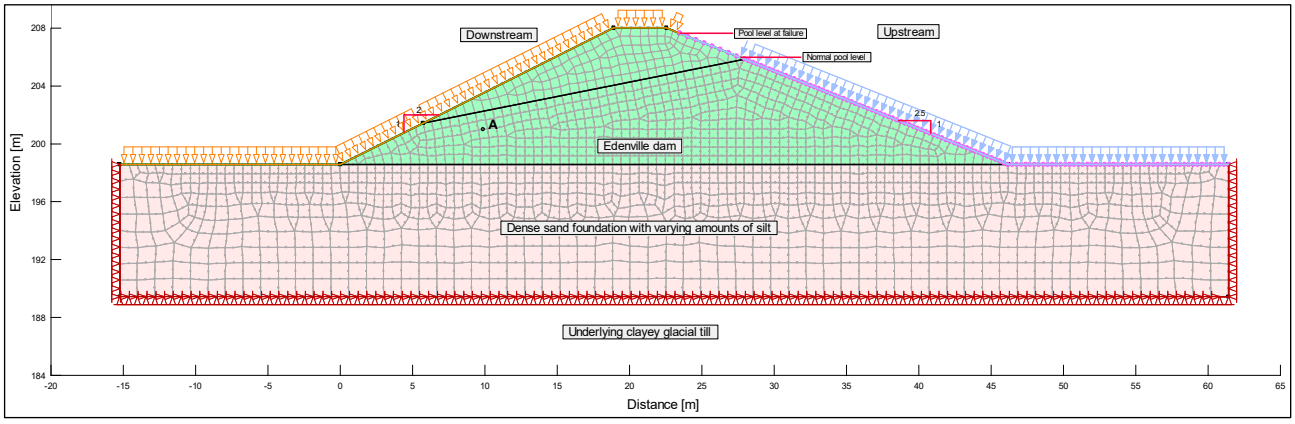

Figure 1. Geometry and meshing of the domain

Step 4 of the modelling sequence presented in Table 1 reproduces the reservoir level behind Edenville dam, during the rainfall event that led to failure. The modelled reservoir level with respect to time is shown in Figure 2. The levels and times used are those reported by the IFT.

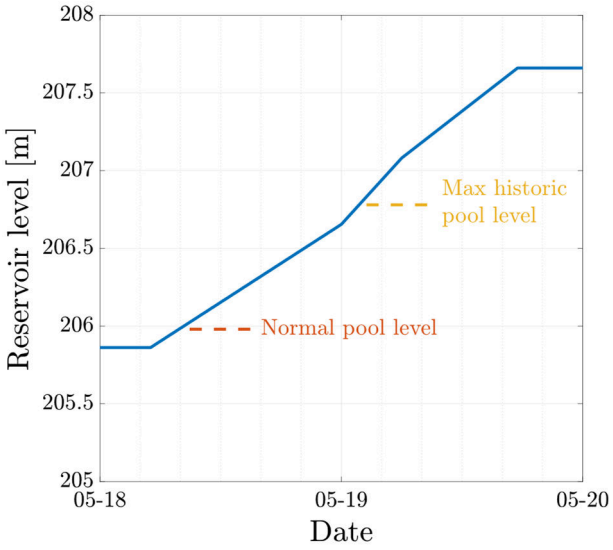

Figure 2. Reservoir level increase during the rainfall event

The simulation starts at midnight on May 18th. The reservoir level is then slightly below the normal operational pool level, at 205.86 m. At 5:00 AM that day, the reservoir level begins to rise. At midnight on May 19th, the reservoir level reaches 206.65 m, which was 0.67 m above the normal operational pool level, and just 0.13 m below the maximum historic pool level (recorded in 1929). The reservoir level continues to increase on May 19th, surpassing the maximum historic pool level, and reaching a maximum elevation of 207.66 m when failure occurred at 5:35 PM that day.

A constant water flux boundary condition is applied to the downstream face and the top of the dam to simulate the precipitations recorded at the site during the rainfall event. These precipitations will infiltrate into the dam and influence the seepage conditions, mainly in the unsaturated zone above the water table. The IFT reports 78.8 mm of rainfall on the day of the 18th and 8.2 mm on the 19th, which correspond to water fluxes of 9.05 and 9.41 $m^3/sec/m^2$ respectively. These values were uniformly applied for each simulated day.

3.3 Soil models and input parameters

Based on the limited information provided by the IFT, only two soil models are used to simulate soils in the domain. This is a simplified approach, which supposes the dam to be homogeneous.

The NorSand constitutive law (Jefferies, 1993) is used to model the dam body (dark green material in Figure 1). NorSand was chosen for its ability to simulate a large variety of sand behaviours, including static liquefaction, which is the focus of this paper. The IFT reports "the most plausible principal mechanism for the failure of Edenville Dam, with strong evidence, is static liquefaction (flow) instability of saturated, loose sands in the downstream section of the embankment." NorSand has successfully been used in other study cases (notably, Shuttle et al. 2022) to simulate static liquefaction.

The underlying foundation is reported to be a dense sand with varying amounts of silt by the IFT. It can be expected that the foundation will be much stiffer than the dam body. The hypothesis is made that most of the important deformations are likely to occur in the dam body. As such, the dense foundation is simulated using an isotropic elastic material model, for simplicity.

The input parameters used for the NorSand and isotropic elastic materials used in the study are shown in Table 3. The NorSand input parameters were adjusted based on comparison results with laboratory data shown in section 4.1, while the isotropic elastic material inputs represent a dense sand.

Table 3. Input parameters for the NorSand and isotropic elastic soil models

Input parameters	Dam body – *NorSand*	Foundation – *Isotropic elastic*
Initial state		
γ	$17\ kN/m^3$	$20\ kN/m^3$
e	0.905	0.60
OCR	1.0	
Elasticity		
ν	0.2	0.3
G_0	$50\ MPa$	$150\ MPa$
m	0.5	
Critical state line		
Γ	0.90	
λ	0.02	
Plasticity		
M_{tc}	1.24	
χ_{tc}	4.5	
N	0.5	
H_0	100	
H_y	0	
S	0.5	

The dam body is simulated as a saturated/unsaturated material, since unsaturated flow will occur above the water table within the dam. Conversely, the foundation is simulated as a saturated-only material since it is unlikely unsaturated flow develops in this zone. Since no information was made available by the IFT about the hydraulic flow properties of the dam material or the foundation, plausible estimates based on values proposed by Carsel and Parrish (1988) are made regarding the input parameters used (shown in Table 4). SEEP/W's built-in estimation functions are used to estimate both the volumetric water content and horizontal hydraulic conductivity functions used for the saturated/unsaturated model of the dam material (shown in Figure 3).

Table 4. Input parameters for hydraulic flow models

Input parameters	Dam body – *Sat./Unsat.*	Foundation – *Saturated*
Saturated horizontal hydraulic conductivity [m/s]	$8.25(10^{-5})$	$5.0(10^{-6})$
Saturated volumetric water content [-]	0.43	0.35
Compressibility [kPa^{-1}]	$1.0(10^{-4})$	$1.0(10^{-6})$

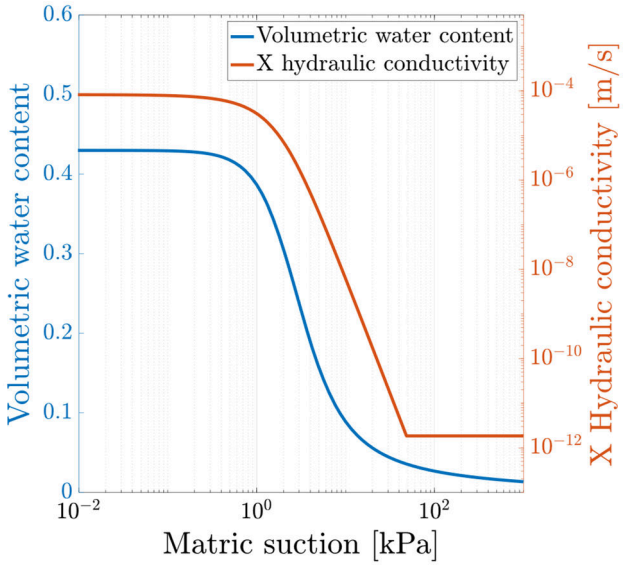

Figure 3. Volumetric water content and horizontal hydraulic conductivity of the dam material

4 SIMULATION RESULTS

4.1 NorSand fit *vs* laboratory results

In their preliminary report, the IFT provides triaxial compression test results from laboratory tests carried out on sand samples retrieved from the Edenville dam embankments. These results comprise three drained and three undrained triaxial compression tests, carried out at an initial relative density of 30%, for various initial confining pressures. This low density is seen as representative of the low compacity that was reported to exist within the dam embankment, where low SPT blow counts were measured.

Figure 4 shows the triaxial compression test results provided in the IFT report (dashed lines). Each color represents a different initial confining pressure. Drained tests are shown in sections A and B of the figure, while undrained tests are shown in sections C and D. Also shown in Figure 4 are the NorSand simulation results (plain lines) matching the laboratory results provided by the IFT. Using the NorSand input parameters shown in Table 4, NorSand compares quite favorably with the laboratory test results.

NorSand's input parameters were adjusted using a trial and error method until the best fit possible was achieved with the laboratory results. This is in no way the best workflow to properly adjust NorSand's input parameters. One would normally prefer dissecting triaxial test results to extract dilatancy trends and locate the critical state locus to properly adjust the model (see Jefferies and Been, 2015, for a thorough description of the preferred method). However, when raw laboratory data is unavailable, such as was the case for this simplified study, trial and error remains a good solution.

In essence, Figure 4 shows an excellent agreement between the laboratory results and the NorSand simulations, irrespective of testing conditions (drained or undrained) and initial confinements. Of crucial importance for this study, the undrained test series (parts C and D of Figure 4) display NorSand's ability to strongly contract when sheared from a loose initial state. The behaviour captured in the laboratory and correctly simulated by NorSand in these tests amounts to static liquefaction. More on that topic in section 5.1.

4.2 Rainfall event

Solving the consolidation analysis which corresponds to the rainfall event (simulation step 4 in Table 1) is the driver of deformations in the simulation. As the reservoir level rises during the rainfall event, the pore-water pressure increases within the dam, which prompts a decrease in mean effective stress and correspondingly, a decrease in general stiffness of the dam.

Figure 5 A reports the vertical displacement of the top right corner of the dam crest as a function of time. Displacements are very small for most of the event, until large deformations start to accumulate at the 1.80-days mark (which corresponds to 19h12 on May 19th). The corresponding available freeboard is plotted in Figure 5 B. At the 1.85-day mark, the available freeboard becomes negative and the simulation is stopped. At this point, the reservoir level is higher than the dam's height, the dam cannot successfully retain the reservoir's content anymore. In other words, the retaining structure has failed to carry out its function.

The pore-water pressure conditions in the dam at the beginning of the rainfall event are contoured in Figure 6 A and can be compared to the conditions at the 1.85-day mark contoured in Figure 6 B. The downstream side of the dam experiences an important increase in pore-water pressure due to the rising free surface inside the dam. An example of such increase is plotted for point A in Figure 7 C (this point is identified in the lower portion of the downstream side of the dam in Figure 6). At this point, the initial pore-water pressure went from 13.1 kPa at the beginning of the rainfall event, to 19.0 kPa at the 1.80-day mark (when excessive deformations began to accumulate), and ended up reaching 38.3 kPa at the 1.85-day mark when the dam failed.

XY deformations at the 1.85-day mark are contoured in Figure 6 C. The corresponding deformed mesh is also shown in red in Figure 6. The upper downstream side of the dam experiences the largest amount of deformations (upward of 0.7 m). The dam crest tilts toward the downstream side of the dam as a result of the large deformations that affect the general downstream portion of the dam.

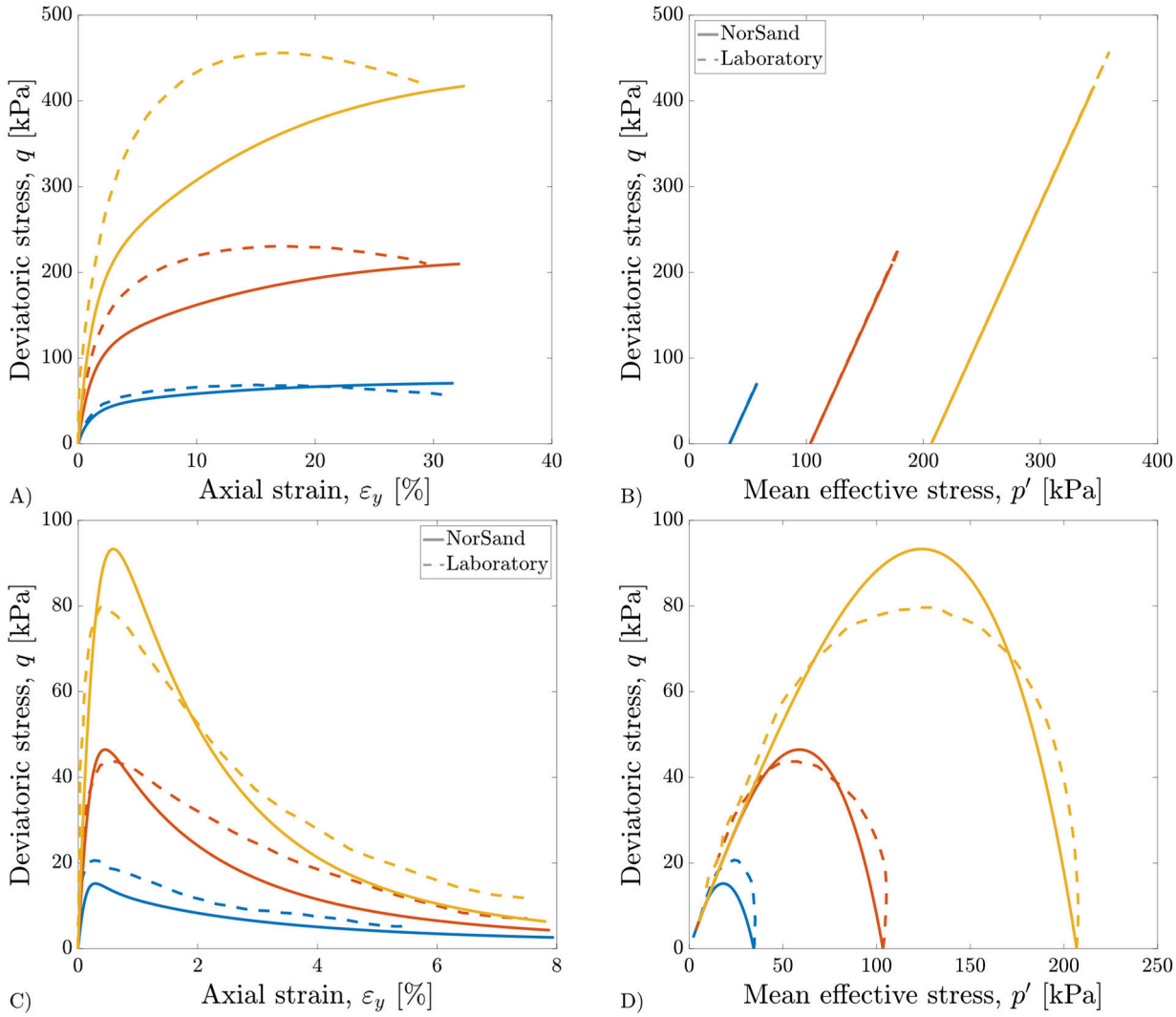

Figure 4. Comparison between drained (A-B) and undrained (C-D) laboratory triaxial compression tests and NorSand

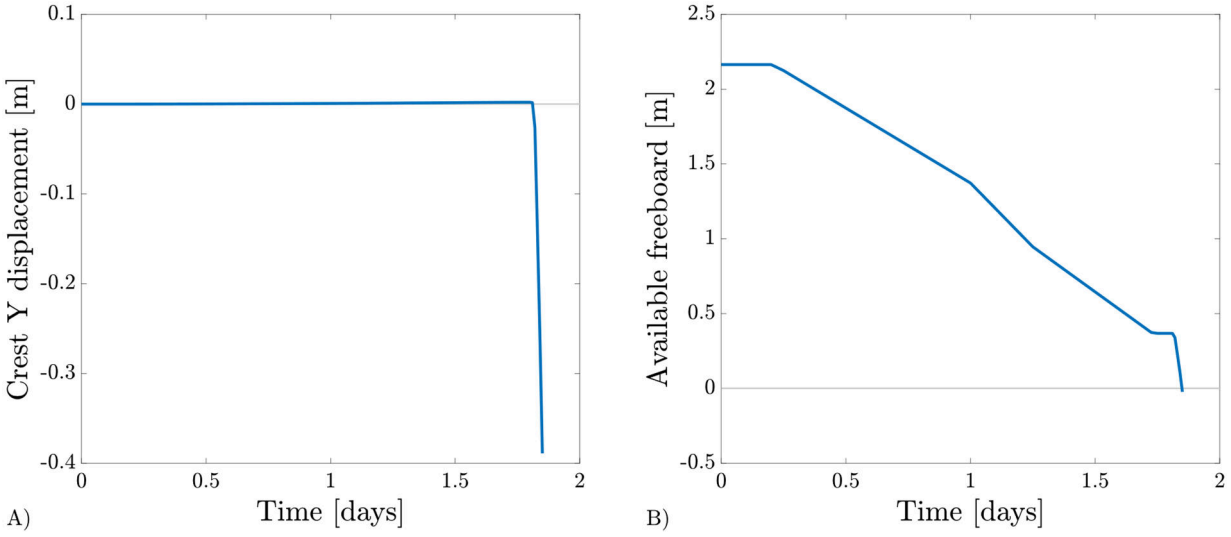

Figure 5. Crest vertical displacement (A) and available freeboard (B) during the rainfall event

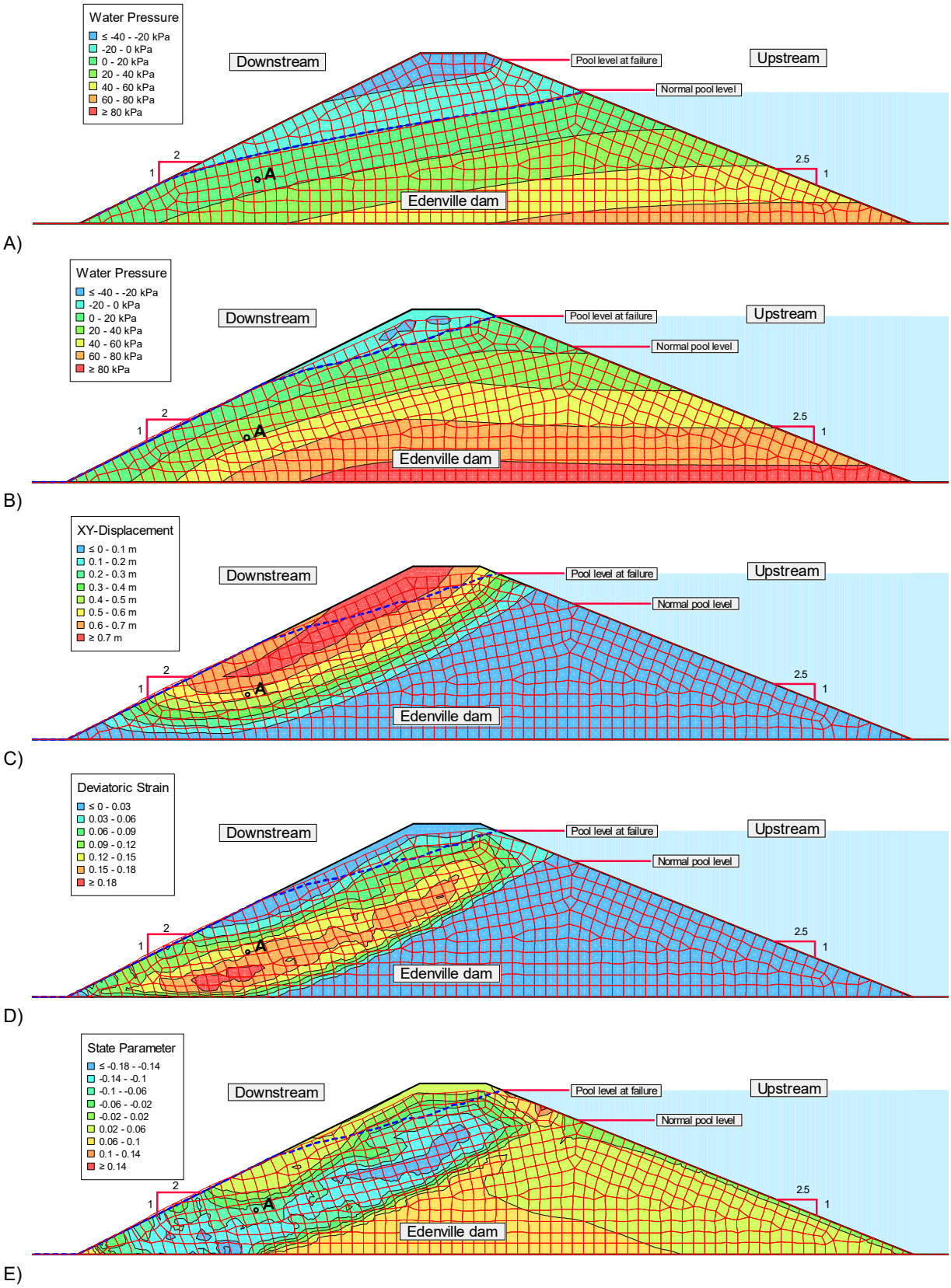

Figure 6. Simulation results at the 1.85-day mark: A) Initial pore-water pressure – B) Final pore-water pressure – C) XY Displacement – D) Deviatoric strain – E) State parameter

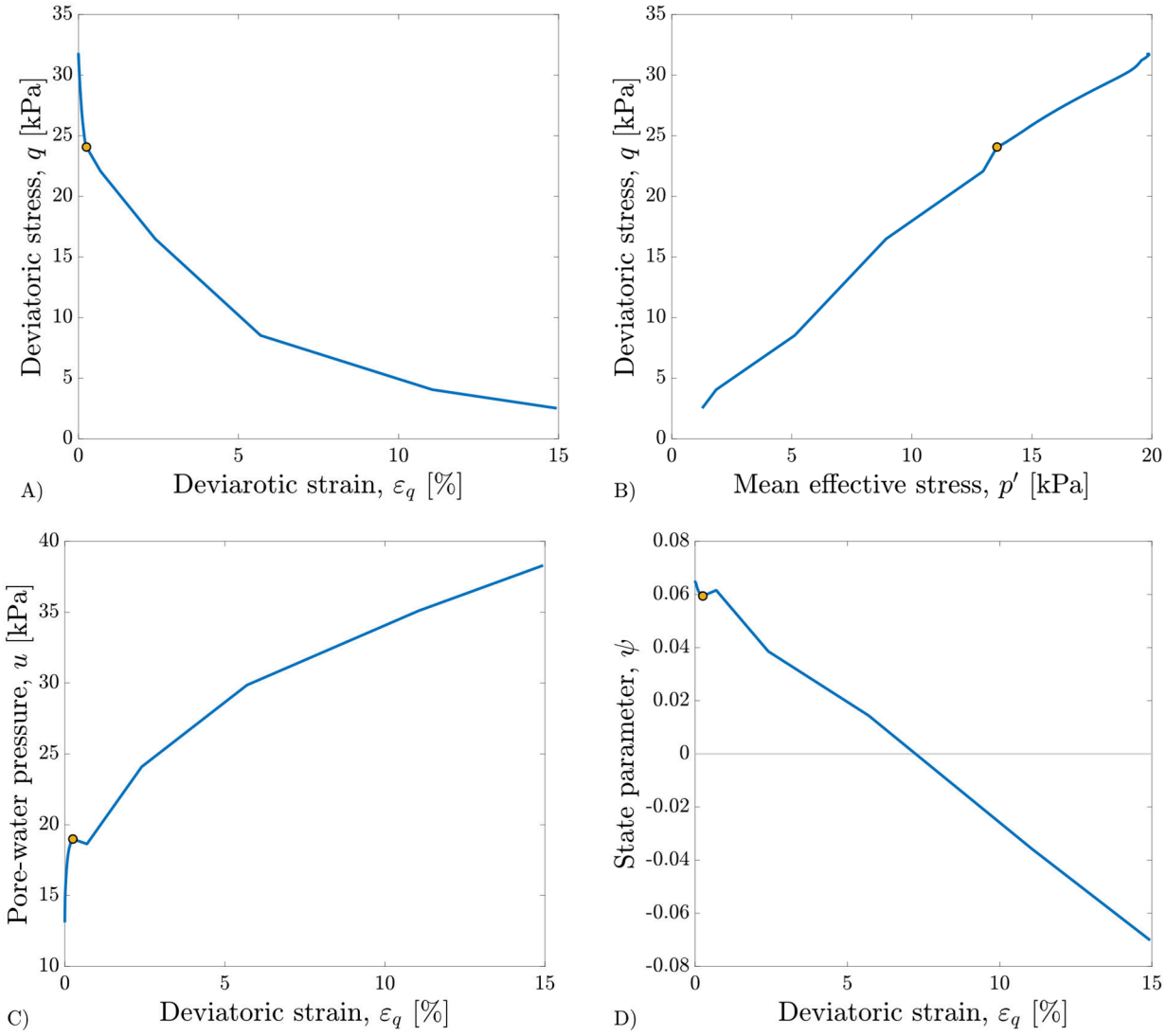

Figure 7. Simulation results at point A at the 1.85-day mark

The large XY deformations shown in Figure 6 C are caused by the shear band that develops in the lower downstream portion of the dam as the water level increases in the reservoir (Figure 6 D). Most of the strains sustained by the dam are concentrated in a band approximately 4 m large, extending from the toe on the downstream side to the area just below the crest on the upstream side. The toe on the downstream side experiences deformations first as the water level increases in the reservoir. Strains exacerbate in this area before extending to the rest of the shear band.

A contour of NorSand's state parameter ψ (Been and Jefferies, 1985) at the 1.85-day mark is shown in Figure 6 E. The state parameter is the difference between the current void ratio and the void ratio at critical state, at constant mean effective stress (see Equation 1). The state parameter is a good indicator of how dense ($\psi < 0$) or loose ($\psi > 0$) a soil is. As shown in Figure 6 E, the upstream side of the dam remains loose after the rainfall event. However, the shear band located on the downstream side contains denser soils. The large deformations sustained by the dam in this zone brought the soils from an initially loose to a denser state (*i.e.* densification occurred).

$$\psi = e - e_c \quad [1]$$

5 DISCUSSION

5.1 Static liquefaction

In *in situ* conditions, static liquefaction can occur in loose soils, most often saturated clean sands, when a perturbation factor induces a reduction in mean effective stress to soils already sustaining some amount of deviatoric stress. These conditions can be met in slopes subjected to an increase in pore-water pressure, such as what was simulated in this study. The unloading brought by

decreasing mean effective stresses can force the stress state onto its yield surface and trigger plastic deformations. If deviatoric stresses were already sufficiently large, that trigger can propel the soil toward static liquefaction, if the soil is loose enough and saturated.

Figure 7 shows the simulation results for point A, labeled in Figure 1 and Figure 6 (lower downstream portion of the dam). As evidenced in section B of the figure (stress path), the deviatoric stress in this area of the dam was already relatively large compared to the mean effective stress. At the start of the rainfall event, the mean effective stress was around 20 kPa and the deviatoric stress was around 32 kPa (stress ratio $\eta = 1.6$). As the pore-water pressure increased, the mean effective stress decreased, which was also accompanied by a deviatoric stress decrease. The yellow point indicated on the figure marks the onset of larger deformations at the 1.80-day mark. Section A of the figure clearly shows how deviatoric strain began rapidly increasing once this threshold was passed. At the yellow point, the pore-water pressure (Figure 7 C) rose very rapidly, which correspondingly brought the mean effective stress down (Figure 7 B). The end result is very low mean effective stresses, which translates into very low shear resistance and very large deformations. Interestingly, the state parameter (Figure 7 D) is propelled past the zero mark as large deformations accumulate (the crossing occurs at around 7 % of deviatoric strain). At this point, the soil is deforming very rapidly, densification occurs as the state parameter drops below zero.

The behaviour described above for point A amounts to static liquefaction. The very brutal and sudden increase in deformation within the shear band eventually leads to large displacements of the dam's crest and even to overtopping. This behaviour matches the video evidence of the failure readily available on the Internet.

5.2 Limitations of the study

This study was purposely conducted with very limited data. The goal was to demonstrate how a simplified numerical simulation can still provide insightful data on deformation mechanisms that might be at work for a given loading scenario. The workflow presented herein proved useful to confirm static liquefaction was indeed possible, given the hypotheses used. The conclusions of such a simplified workflow could be used to inform decisions regarding the next steps to take for an investigation. Some of the main limitations of the study are discussed below and should be taken into account before any conclusions are drawn based on the results presented in this study.

The cross-section of Edenville dam where the failure occurred was reconstructed based on the IFT report. Without any details regarding the inner structures or zones that may exist within the dam, it was supposed homogenous and built of a single material. The void ratio of the sand material was assumed constant and equivalent to the relative density of the samples tested in the laboratory by the IFT. *In situ* investigations using CPTs would prove useful to better define the density (or ideally, the state parameter) that existed in the dam prior to failure.

Water seepage dynamics play a crucial role in any dam-like numerical simulation. How fast or slow the free surface adjusts following an increase in reservoir level is dictated by the saturated and unsaturated flow characteristics of the dam's materials. Without any data to work with, literature values for sands were used as best estimates. Laboratory measurements of hydraulic conductivity and volumetric water content functions would provide insightful data to better adjust the simulations.

6 CONCLUSION

A simple numerical analysis, based on limited data, was performed in this analysis to investigate if static liquefaction was likely to occur at Edenville dam following the intense rainfall event recorded on May 18th and 19th, 2020. A simple cross-section of the dam was modelled in GeoStudio. The NorSand soil model was used to simulate the dam's body material. The constitutive model was calibrated on triaxial test results made available by the IFT. The effect of the rainfall event was simulated via infiltration on the downstream side of the dam and reservoir level increase on the upstream side of the dam. The consolidation analysis performed revealed a stable behaviour until the 1.80-day mark was passed (approximately 19h12 on May 19th). The deformations within the dam rose quickly after this point. Static liquefaction within the large shear band that developed in the lower downstream side of the dam was identified as the main driver of large deformations. At the 1.85-day mark, the upstream side of the dam crest fell below the reservoir level and the numerical simulation was stopped. Many hypotheses were proposed to conduct this simplified study. Its results could nevertheless help decision-makers choose a path forward in selecting appropriate *in situ* and laboratory investigation tools to confirm the likelihood of static liquefaction as the cause of rupture for Edenville dam.

7 REFERENCES

Been, K. and Jefferies, M. G. 1985. A state parameter for sands. *Géotechnique*, 32(2): 99-112.

Carsel, R. F., Parrish, R. S. (1988). Developing joint probability distributions of soil water retention characteristics. *Water Resources Research*, 24(5): 755-769.

France, J. W., Alvi, I., Williams, J. L., Miller, A., Higinbotham, S. (2021). *Investigation of failures of Edenville and Sanford dam* (Independent Forensic Team Interim Report). Federal Energy Regulatory Commission.

Jefferies, M. G. (1993). Nor-Sand: A simple critical state model for sand. *Géotechnique*, 43(1): 91-103.

Jefferies, M. and Been, K. 2016. *Soil liquefaction: A critical state approach*, 2nd edition, CRC Press.

Seequent (2022). GeoStudio, version 2022.1. Retrieved from http:www.geoslope.com.

Shuttle, D., Marinelli, F., Brasile, S., Jefferies, M. (2022). Validation of computational liquefaction for tailings: Tar Island slump. *Geotechnical Research*, 9(1): 32–55.